

Thermoanalytical characterization of herbal drugs from *Poincianella pyramidalis* in different particle sizes

Geovani Pereira Guimarães^{1,2} · Ravelly Lucena Santos^{1,2} ·
Deysiane Oliveira Brandão^{1,2} · Nathália Alexandra de Oliveira Cartaxo-Furtado^{1,2} ·
Airla Laana de Medeiros Cavalcanti³ · Rui Oliveira Macedo^{1,2}

Received: 21 May 2016 / Accepted: 19 December 2016 / Published online: 12 January 2017
© Akadémiai Kiadó, Budapest, Hungary 2017

Abstract *Poincianella pyramidalis* (Tul.) L.P. Queiroz, known as “catingueira,” is a typical species of Caatinga and used in Brazilian folk medicine as anti-inflammatory, anti-pyretic, diuretic and expectorant. Pharmacological analyses confirmed his activity as anti-inflammatory, antimicrobial and in gastrointestinal disorders. This paper aimed to perform a thermoanalytical characterization of the herbal drugs obtained from *P. pyramidalis* leaves in different particle sizes. The leaves were dried, pulverized and separated into different granulometric ranges: 50–100, 100–200, 200–400 and <400 mesh. The samples were characterized by thermogravimetry (TG) at different atmospheres and heating rates, determination of the kinetic degradation parameters by Ozawa model, differential thermal analysis (DTA), pyrolysis coupled to gas chromatography interfaced with mass spectrometry (Pyr-GC/MS) and multivariate analysis. TG curves of the samples showed the presence of six thermal decomposition events, with greater mass loss (25.91–35.66%) in the range of 247–398 °C. The thermal degradation proved to be a reaction of zero order, with a decrease in enthalpy and frequency factor with decreasing the granulometric range. DTA curves showed three exothermic events, with peaks around 350, 460 and 490 °C, with variation in enthalpy values. With the Pyr-GC/

MS were evidenced different profiles according to the temperature. Principal component analysis of pyrolysis data from samples at different temperatures was able to represent the total variability within the first two principal components, revealing differences between the granulometric ranges. The analytical and statistical techniques used were able to trace characteristic profiles of the herbal drugs, elucidating the differences in each granulometric range.

Keywords *Poincianella pyramidalis* · TG · DTA · Degradation kinetics · Pyrolysis · PCA

Abbreviations

TG	Thermogravimetry
DTA	Differential thermal analysis
Pyr-GC/MS	Pyrolysis coupled to gas chromatography interfaced with mass spectrometry
PCA	Principal component analysis
HCA	Hierarchical cluster analysis
ACAM	Manuel de Arruda Câmara herbarium
β	Heating ratio
n	Reaction order
E_a	Activation energy
A	Frequency factor
EI	Electron impact
m/z	Mass-to-charge ratio
T_{onset}	Initial temperature
T_{endset}	Final temperature

Introduction

The use of herbs and other natural products with therapeutic properties has been globally appreciated due to factors such as the search for healthier living habits and

✉ Geovani Pereira Guimarães
geovanipguimaraes@gmail.com

¹ Graduate Program in Pharmaceutical Sciences, Federal University of Pernambuco, Recife, PE, Brazil

² Unified Laboratories of Pharmaceutical Development and Assays, Department of Pharmaceutical Sciences, Federal University of Paraíba, Campus I, University City, João Pessoa, PB 58059-970, Brazil

³ Pharmacy Department, State University of Paraíba, Campina Grande, PB, Brazil

difficulties in the conventional treatment of certain diseases [1]. Medicinal herbs are promising therapeutic agents due to the diversity of chemical compounds they produce, such as secondary metabolites that often exhibit pharmacological properties [2]. It is estimated that in the USA and the UK the annual average use of herbal drugs-based products in complementary alternative medicine is 25 and 41.1%, respectively [3].

Poincianella pyramidalis (Tul.) L.P. Queiroz, known as “catingueira”, is a typical species of Caatinga, a semiarid region from Brazil, and used in folk medicine as anti-inflammatory, antipyretic, diuretic and expectorant [4]. Pharmacological properties like antimicrobial activity against multidrug-resistant *Staphylococcus aureus* [5]; gastroprotective activity and antimicrobial activity against *Helicobacter pylori* [6]; anti-inflammatory action and antinociceptive [7, 8] have already been proven to this species. The presence of secondary metabolites with known antimicrobial activity such as the ursolic acid, quercetin, catechins, ellagic acid, sitosterol, proanthocyanidins and gallic acid [9] can be associated with its pharmacological properties. Also was confirmed the presence of flavonoids, biflavonoids, phenylpropanoids, lupeol, lignin, chalcone and triterpenes [6]. The pharmacological and chemical profiles make *P. pyramidalis* a potential source for use in the pharmaceutical field, such as in herbal drugs.

Due to its complex composition, herbal drugs require special methods and strategies to verify your quality and integrity [10]. Thermal analyses such as thermogravimetry (TG) and differential thermal analysis (DTA) are techniques of high sensitivity, reproducibility and rapid response to variations in mass and enthalpy, obtaining results related to the composition and thermal stability of the sample [11]. The Ozawa kinetic model obtained from the dynamic TG data was already used to differentiate pharmaceutical raw material such as herbal drugs. Pyrolysis coupled to gas chromatography interfaced with mass spectrometry (Pyr-GC/MS) associated with thermal analysis is a useful tool in the comprehension of chemical composition and products of the thermal decomposition of materials. Multivariate data analysis methods such as principal component analysis (PCA) and hierarchical cluster analysis (HCA) are useful statistic tools for recognizing patterns in the investigated information sets by increasing the understanding of data, verifying the presence or absence of natural groupings of samples [12].

This paper aimed to develop an analytical model to characterize powdered herbal drugs in different particle sizes obtained from the leaves of *P. pyramidalis* in order to establish specifications for quality control of the herbal pharmaceutical active ingredient.

Materials and methods

Raw material

The raw material used (leaves) was harvested in the municipality of Coxixola, Paraíba, Brazil (7°37'31"S, 36°36'12"W), during July 2014. The plant was identified as *Poincianella pyramidalis* (Tul.) L.P. Queiroz by comparison with voucher number 039/ACAM stored in the Manuel de Arruda Câmara (ACAM) herbarium.

Powder preparation

The leaves were dehydrated in a solar dryer developed by the company TELAB[®] (Technologies for Laboratories and Bioprocess LTDA, Brazil) for 4 days. The dried leaves were milled using a combined hay cutter machine (TFC 150, LABOREMUS[®], Brazil). The different particle sizes were separated using a vibration separator (GY-600-35A, Guan Yu Machinery Factory Co., China) with distinct steel sieves with openings of 50, 100, 200 and 400 mesh, respectively, 297, 149, 74 and 37 μm . The herbal drugs obtained by each mesh was classified into four groups according to their granulometric range (50–100, 100–200, 200–400 and <400 mesh) and stored in a frosted white polyethylene container, properly sealed and protected from light and humidity at room temperature.

Characterization of the herbal drugs

Characterization of the herbal drugs was performed based on thermoanalytical, chromatographic and multivariate analysis.

Thermogravimetric analysis (TG)

The dynamic thermogravimetric curves of the different samples were obtained in a thermobalance (TGA-50, Shimadzu[®], Japan) using an alumina crucible. The instrument was calibrated with calcium oxalate monohydrate. The temperature range used was 35–900 °C in the heating ratios (β) of 5, 10, 20 and 40 °C min^{-1} under synthetic air atmosphere and 10 °C min^{-1} under nitrogen atmosphere, with flow of 20–50 mL min^{-1} , respectively. The sample mass was 5.0 ± 0.1 mg. Data were initially analyzed using the software TA 60 WS (Shimadzu[®], Japan), and the determination of the temperature range (start and end) to obtain the mass loss percentual of each step was obtained by the tangent method. The TG curves were plotted using Origin[®] Pro 8.0 (OriginLab Research).

Kinetic parameters determination

The reaction order (n), activation energy (E_a) and frequency factor (A) were determined using the Ozawa model with the data of dynamic TG in atmosphere of synthetic air (5, 10, 20 and 40 °C min⁻¹) using the software TA-50 (TGA Kinetic Analysis Application, Shimadzu[®], Japan).

Differential thermal analysis (DTA)

The DTA curves of the samples were obtained using a differential thermal analyzer (model DTA-50, Shimadzu[®], Japan) in nitrogen atmosphere (50 mL min⁻¹) at a heating rate of 10 °C min⁻¹, from 35 °C up to the temperature of 900 °C. The samples were analyzed using the TA 60 WS software (Shimadzu[®], Japan). The samples mass was 5.0 ± 0.1 mg. The apparatus was calibrated through the melting points of the standards zinc and indium. The DTA curves were plotted using Origin Pro 8.0 (OriginLab[®] Research).

Pyrolysis coupled to gas chromatography interfaced with mass spectrometry (Pyr-GC/MS)

The pyrolyzer (Pyr-4A, Shimadzu[®], Japan) was directly interfaced with a gas chromatograph/mass spectrometer (GCMS-QP5050A, Shimadzu[®], Japan). A capillary column with stationary phase phenyl/dimethylpolysiloxane (5:95) was used (with 30 m length, 0.25 mm internal diameter and 0.25 µm particle size). The gas chromatograph was interfaced with the mass spectrometer, which was configured to scan a mass range from m/z 50 to 450. Helium was used as carrier gas at a flow rate of 1.5 mL min⁻¹ and a 1:5 split ratio. The interface temperature was set at 300 °C. Ionization was effected by electron impact (EI) at 70 eV. The chromatographic run was performed using a temperature ramp at the rate 15 °C min⁻¹, starting at 70 up to 300 °C, and being held for 5 min. A fraction of the samples in the platinum crucible was introduced in the pyrolyzer preheated at temperatures of 250, 350 and 450 °C, separately for each experiment. The identification of the compounds was made by comparison of their mass spectra with the Wiley/NBS library reference data. The pyrograms were plotted using Origin Pro[®] 8.0 (OriginLab[®] Research).

Multivariate analysis

Principal component analysis (PCA) and hierarchical cluster analysis (HCA) were implemented using XLSTAT software (Addinsoft[®], New York, USA) to the Pyr-GC/MS data. The peaks selected from the pyrograms for each temperature were integrated, and their values of area were

treated by self-scaling, subtracting individual peak area values of their respective average and then dividing this value by the standard deviation computed from the different areas. After this treatment, the correlating matrix of the samples (particle sizes) was generated with the variables (identified compounds during pyrolysis). To perform the PCA, the Pearson correlation matrix was used, resulting in graphs for the principal components for samples and variables. For the HCA, the dissimilarity coefficient used was the Euclidean distance, which generated distinct dendrograms for the clustering of samples and variables.

Results and discussion

Figure 1 shows the thermogravimetric curves of the *P. pyramidalis* herbal drugs subjected to the same heating rate (10 °C min⁻¹) in different atmospheres (synthetic air and nitrogen). The thermal decomposition of the samples in both atmospheres occurred in six stages. In the presence of synthetic air, the herbal drugs showed a more marked decomposition, with less non-degradable residue formation and a characteristic aspect of incinerated material. When in an inert atmosphere, the residual mass was greater in percentage, and it presented an aspect of incomplete combustion.

The first stage of thermal decomposition in synthetic air atmosphere occurred at the temperature range and equivalent mass loss of 35–87.9 °C (5.30%), 35–91.86 °C (5.07%), 35–91.81 °C (5.07%) and 35–89.93 (5.40%) for *P. pyramidalis* herbal drugs 50–100, 100–200, 200–400 and <400 mesh, respectively. In nitrogen atmosphere, the same event was observed at 35–98.58 °C (6.1%), 35–105.26 °C (6.5%), 35–93.43 °C (5.5%) and 35–90.27 °C (5.85%). This stage is characterized by the loss of volatile compounds, particularly free water. The second step refers mainly the loss of bound water, presenting similar mass loss values to all samples in all conditions. The following steps represent the micro- and macro-components degradation.

Figure 2 shows the TG curves obtained for the samples in a synthetic air atmosphere in different heating rates (5, 10, 20 and 40 °C min⁻¹). It was observed the presence of six events of thermal decomposition, described in Table 1. There was a shift in the initial and final temperatures (T_{onset} and T_{endset}) of the events with an increasing heating rate and the increase in mass loss values of the samples. This shift relates to the difference in the heat transfer rate to the sample; there are different temperature gradients between the surface and the interior of the herbal drug particles with each heating rate [13].

For all samples evaluated, the fourth stage presented the greatest mass loss values in a synthetic air atmosphere (Table 1). Thus, this stage was considered the principle

Fig. 1 TG curves of *P. pyramidalis* herbal drugs submitted to different atmospheres

($\beta = 10\text{ }^{\circ}\text{C min}^{-1}$).

a *P. pyramidalis* 50–100 mesh;

b *P. pyramidalis* 100–200 mesh;

c *P. pyramidalis* 200–400 mesh;

d *P. pyramidalis* <400 mesh

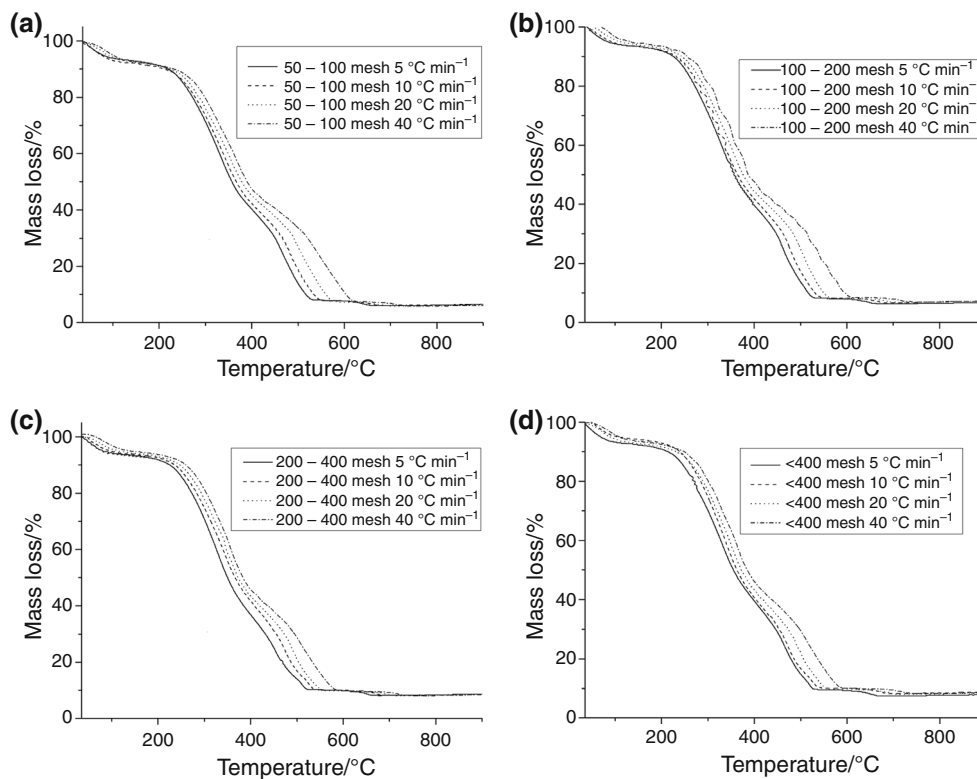
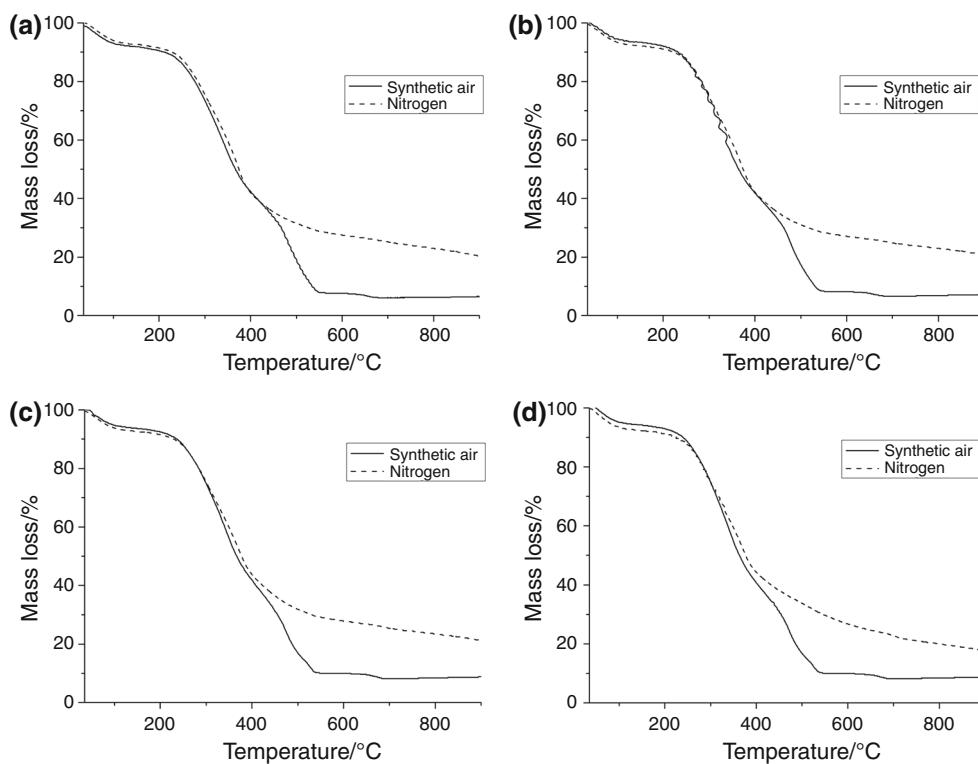


Fig. 2 TG curves of *P. pyramidalis* herbal drugs in synthetic air atmosphere and in different heating rates. **a** *P. pyramidalis* 50–100 mesh; **b** *P. pyramidalis* 100–200 mesh; **c** *P. pyramidalis* 200–400 mesh; **d** *P. pyramidalis* <400 mesh

Table 1 Description of the six stages of thermal decomposition in a synthetic air atmosphere

<i>P. pyramidalis</i> herbal drugs	Heating rate/ °C min ⁻¹	1			2			3		
		<i>T</i> _{onset} / °C	<i>T</i> _{endset} / °C	Mass loss/ %	<i>T</i> _{onset} / °C	<i>T</i> _{endset} / °C	Mass loss/ %	<i>T</i> _{onset} / °C	<i>T</i> _{endset} / °C	Mass loss/ %
50–100 mesh	5	35.00	85.60	5.14	85.60	208.23	3.85	208.23	261.45	6.16
	10	35.00	87.93	5.30	87.93	224.39	4.61	224.39	267.07	6.56
	20	35.00	103.66	5.52	103.66	229.33	4.45	229.33	288.86	10.06
	40	35.00	126.08	6.46	126.08	244.86	3.76	244.86	294.23	8.09
100–200 mesh	5	35.00	80.94	4.88	80.94	194.89	3.07	194.89	247.59	5.58
	10	35.00	91.86	5.07	91.86	214.94	3.61	214.94	256.11	5.03
	20	35.00	101.55	5.14	101.55	222.43	3.73	222.43	265.56	4.94
	40	35.00	110.89	5.16	110.89	236.11	3.90	236.11	291.89	8.81
200–400 mesh	5	35.00	77.70	4.68	77.70	205.48	3.71	205.48	259.02	7.59
	10	35.00	91.81	5.07	91.81	216.25	3.50	216.25	287.41	12.56
	20	35.00	102.95	4.62	102.95	227.92	3.81	227.92	293.60	11.45
	40	35.00	118.21	5.14	118.21	235.20	3.43	235.20	295.99	9.39
<400 mesh	5	35.00	87.65	5.73	87.65	196.44	2.65	196.44	264.13	9.31
	10	35.00	89.93	5.40	89.93	208.59	3.14	208.59	272.51	8.92
	20	35.00	97.28	5.26	97.28	216.74	3.44	216.74	278.57	7.98
	40	35.00	106.60	4.69	106.60	232.24	4.19	232.24	290.09	7.98
<i>P. pyramidalis</i> herbal drugs	Heating rate/ °C min ⁻¹	4			5			6		
		<i>T</i> _{onset} / °C	<i>T</i> _{endset} / °C	Mass loss/ %	<i>T</i> _{onset} / °C	<i>T</i> _{endset} / °C	Mass loss/ %	<i>T</i> _{onset} / °C	<i>T</i> _{endset} / °C	Mass loss/ %
50–100 mesh	5	261.45	377.53	<i>37.05</i>	377.53	467.34	17.05	467.34	539.94	20.90
	10	267.07	380.63	<i>36.49</i>	380.63	475.97	19.46	475.97	549.14	19.12
	20	288.86	384.47	<i>31.07</i>	384.47	487.22	17.39	487.22	564.58	22.21
	40	294.23	394.85	<i>32.45</i>	394.85	514.66	17.59	514.66	613.00	23.29
100–200 mesh	5	247.59	364.93	<i>38.18</i>	364.93	450.50	18.75	450.50	525.47	20.81
	10	256.11	368.89	<i>37.28</i>	368.89	457.78	17.60	457.78	536.33	22.19
	20	265.56	380.43	<i>37.31</i>	380.43	484.63	18.57	484.63	554.61	20.65
	40	291.89	397.09	<i>34.57</i>	397.09	511.14	17.03	511.14	603.79	21.84
200–400 mesh	5	259.02	363.05	<i>37.59</i>	363.05	424.85	13.80	424.85	520.28	21.10
	10	287.41	371.56	<i>30.08</i>	371.56	460.61	19.62	460.61	535.90	18.05
	20	293.60	378.39	<i>31.50</i>	378.39	474.90	18.73	474.90	548.25	18.95
	40	295.99	383.47	<i>32.33</i>	383.47	485.70	17.88	485.70	575.19	20.86
<400 mesh	5	264.13	356.02	<i>32.00</i>	356.02	450.08	20.61	450.08	525.55	18.88
	10	272.51	367.06	<i>34.21</i>	367.06	468.51	22.30	468.51	534.31	14.93
	20	278.57	383.36	<i>35.90</i>	383.36	478.26	18.42	478.26	542.22	16.82
	40	290.09	387.01	<i>33.74</i>	387.01	489.08	17.57	489.08	578.48	20.70

The values are in italics to emphasize that they represent the largest mass loss of all stages

stage of thermal decomposition, and it served as a reference for obtaining the kinetic parameters of thermal degradation by the Ozawa method.

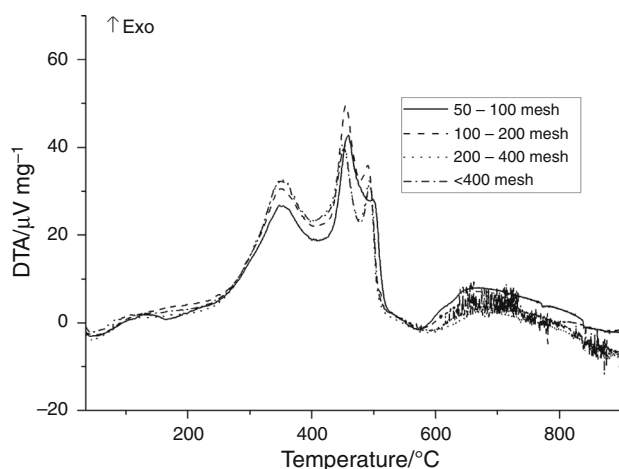
Table 2 shows the data obtained through the application of Ozawa's kinetic model during the evaluation of the fourth degradation event. The thermal decomposition of the samples presented as a zero-order reaction. Correia et al. [11] observed that behavior when evaluated the degradation kinetics of *Tabebuia caraiba* herbal drugs in

conditions similar to those of the present study. The values of E_a and A presented decreased as a function of the granulometric range. The herbal drugs with larger particle sizes need more energy to promote the enthalpic events related to their thermal decomposition.

To all herbal drugs were observed three exothermic peaks in the differential thermal analysis curves (Fig. 3), described in terms of temperature and enthalpy (Table 3).

Table 2 Kinetic degradation parameters of *P. pyramidalis* herbal drugs using the Ozawa method

<i>P. pyramidalis</i> herbal drugs	Kinetic parameters	
	Activation energy/J mol ⁻¹	Frequency factor/min ⁻¹
50–100 mesh	200,620 ± 1390	5.22 × 10 ¹⁵
100–200 mesh	192,640 ± 12,380	9.06 × 10 ¹⁴
200–400 mesh	186,170 ± 9670	4.43 × 10 ¹⁴
<400 mesh	180,180 ± 10,720	1.06 × 10 ¹⁴

**Fig. 3** Differential thermal analysis curves of *P. pyramidalis* herbal drugs

The first peak occurred in a temperature interval covered by the fourth thermal decomposition event, near to 350 °C. This event presented the highest values of enthalpy for all the evaluated herbal drugs. The third peak presented the smaller values of enthalpy, appearing as an unfolding of the second peak.

Data from TG and DTA were selected for the evaluation of the degradation products of the samples by Pyr-GC/MS analysis at representative temperatures of the initial (250 °C) and intermediate (350 and 450 °C) degradation stages of the macro- and microconstituent processes. The herbal drugs presented different profiles depending on the temperature, due to the number of released compounds. At a given temperature, the same compounds were released,

but differing in their intensity values and area, features directly related to the concentration. The peaks are identified by their degree of similarity by comparing their mass spectra with the Wiley/NBS library reference data.

At 250 °C (Fig. 4a), fewer peaks occurred. The following compounds were identified by their retention times (min): 3-nonynoic acid (14.5); oleic acid (17.4); 8,11,14-eicosatrienoic acid (17.9); hexadecanoic acid (22.4); squalene (23.5); pentatriacontane (24.0) and alpha tocopherol (26.9). At the temperature of 350 °C (Fig. 4b), a greater amount of compounds was evidenced. In common with the previous temperature was observed the presence of hexadecanoic, oleic and 8,11,14-eicosatrienoic acid, squalene and alpha tocopherol, featuring the continuity of the thermal decomposition process shown in the above temperature. The other compounds identified were: 2-(1,1-dimethylethoxy)-5-(methyl-D3) thiophene (8.1); 3-methyl-2-(2-methyl-2-butenyl)-furan (8.2); eugenol (10.0); 2,4,4-trimethyl-3-carboxaldehyde-5-hydroxy-2,5-cyclohexadien-1-one (11.6); spiro [androst-5-ene-17,1'-cyclobutan]-2'-one 3-hydroxy-(3.beta.17.beta.) (13.3); neophytadien (14.5); phytol (14.9); farnesyl alcohol (15.4); palmitic acid (16.3); farnesyl acetate (19.9); 1-chlorooctadecane (22.4); geraniol-linalool isomers (23.3); tritetracontane (24.0) and quebrachol (26.7) and may represent new products resulting from the degradation of components at this temperature. In the pyrograms obtained at 450 °C (Fig. 4c) were found more peaks than previous temperatures. It was possible to observe in common with the pyrograms of the preceding temperatures the presence of the compounds 8,11,14-eicosatrienoic acid, squalene and alpha tocopherol. Phytol and quebrachol, compounds identified in the

Table 3 Temperature and enthalpy of the DTA peaks

<i>P. pyramidalis</i> herbal drugs	First peak		Second peak		Third peak	
	$T_{\text{peak}}/^{\circ}\text{C}$	Enthalpy/J g ⁻¹	$T_{\text{peak}}/^{\circ}\text{C}$	Enthalpy/J g ⁻¹	$T_{\text{peak}}/^{\circ}\text{C}$	Enthalpy/J g ⁻¹
50–100 mesh	347.86	646.54	459.39	493.77	498.45	146.67
100–200 mesh	349.67	733.50	455.15	548.14	490.56	251.89
200–400 mesh	351.09	821.35	451.12	475.07	492.41	302.52
<400 mesh	349.37	804.32	451.92	446.13	493.66	242.35

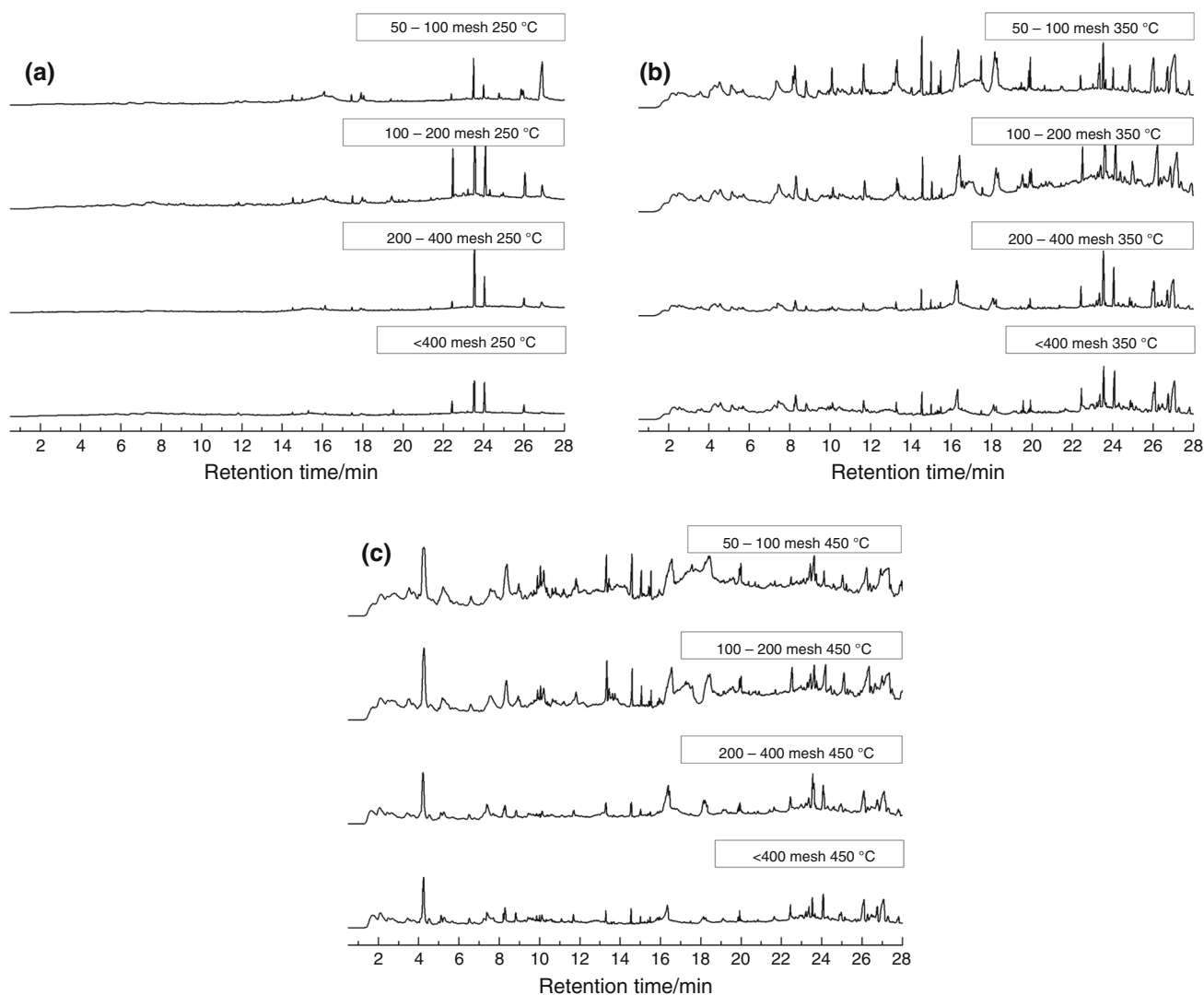


Fig. 4 Pyrograms of *P. pyramidalis* herbal drugs at different temperatures. **a** 250 °C; **b** 350 °C; **c** 450 °C

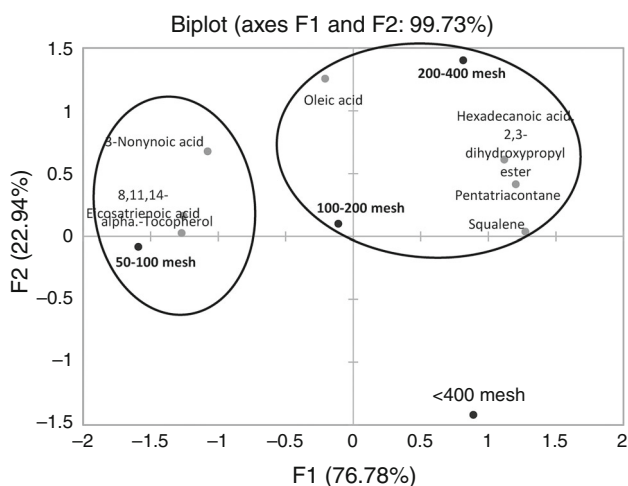


Fig. 5 Biplot of all variables (compounds) and samples at a temperature of 250 °C

pyrograms of 350 °C, were also observed. The other identified compounds were: limonene (4.2); benzyl 3-oxo-5-(1-nitro-2-oxocycloheptyl) pentanoate (7.7); *O*-nitrocyclopropylbenzene (8.4); farnesol (9.8); 1,5,9-decatrien, 2,3,5,8-tetramethyl (10.0); trans-2 (1H)-naphthalenone-3,4,4a, 5,8,8a-hexahydro-4a-methyl (10.2); iso geraniol (10.7); jasmolone (11.8); 7 heptadecene-7-methyl (13.3); trans-caryophyllene (13.4); dolicodial (15.0); farnesol (15.5); tetraeurin-A-diol (18.5); 1,3-6-nitro-cyclohexadecanedione (22.4); nerolidol (23.2); 1-chlorooctadecane (25.0) and caryophyllene oxide (27.3).

Given the complexity of the data generated during pyrolysis, the application of multivariate analysis can be useful for establishing, through graphics, the parameters/variables mainly responsible for the formation of group samples. This analysis allows the establishment of a particular chemical signature for each studied group [14, 15]. Data regarding the average peak area of the

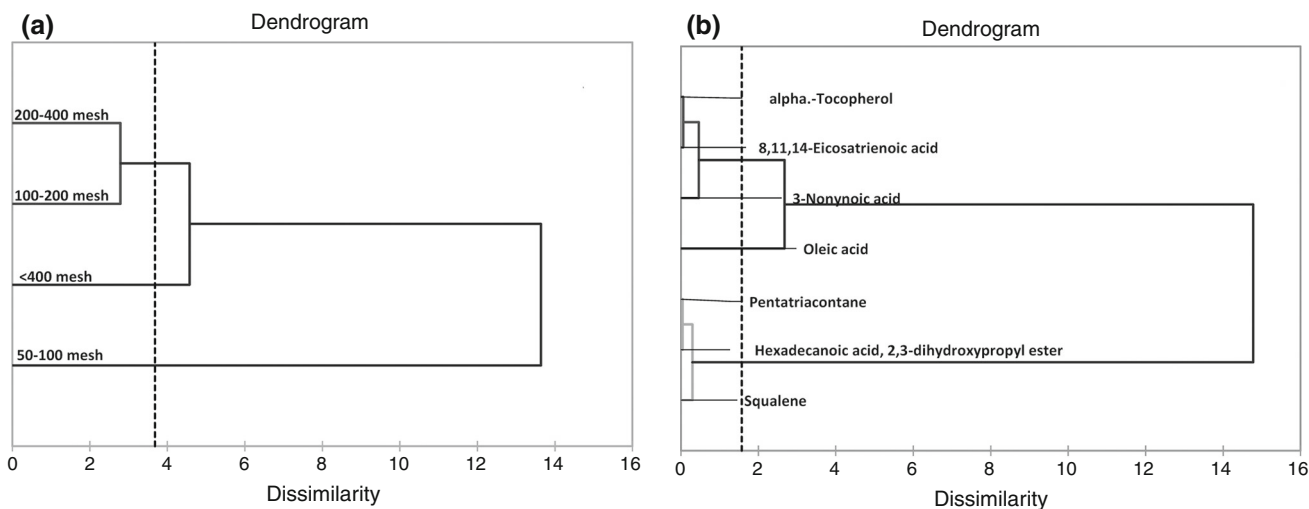


Fig. 6 Dendrograms obtained by HCA of pyrolysis data from the *P. pyramidalis* herbal drugs (a) and compounds (b) at 250 °C

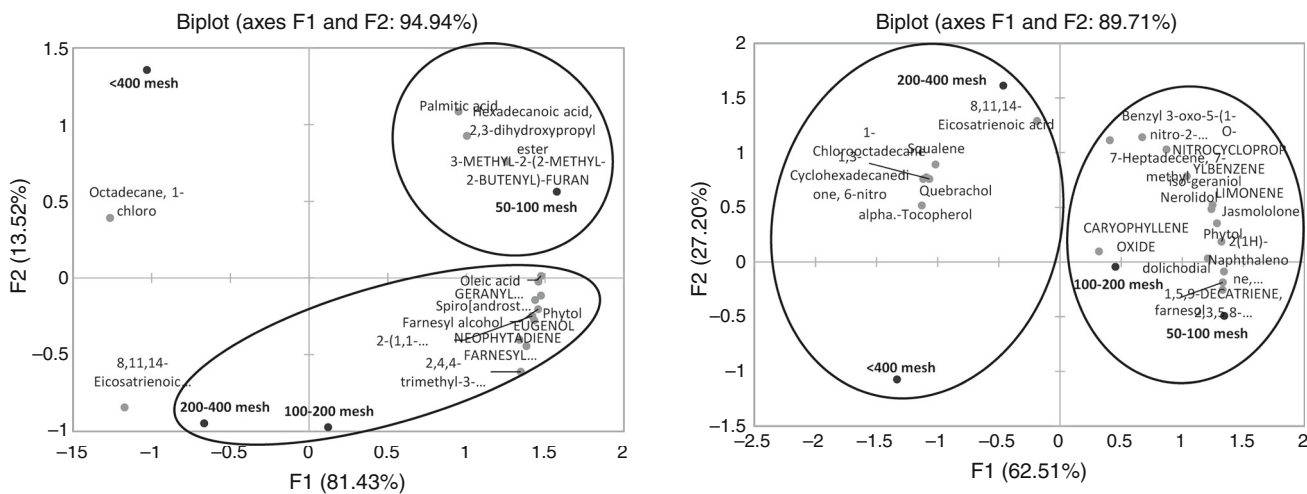


Fig. 7 Biplot of all variables (compounds) and samples at a temperature of 350 °C

Fig. 9 Biplot of all variables (compounds) and samples at a temperature of 450 °C

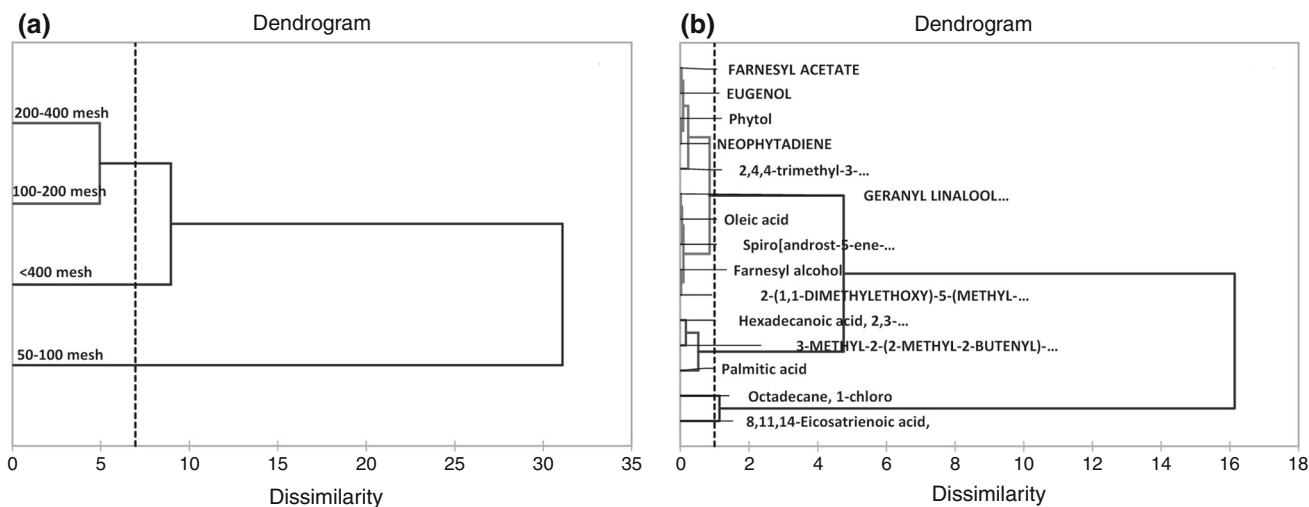


Fig. 8 Dendrograms obtained by HCA of pyrolysis data from the *P. pyramidalis* herbal drugs (a) and compounds (b) at 350 °C

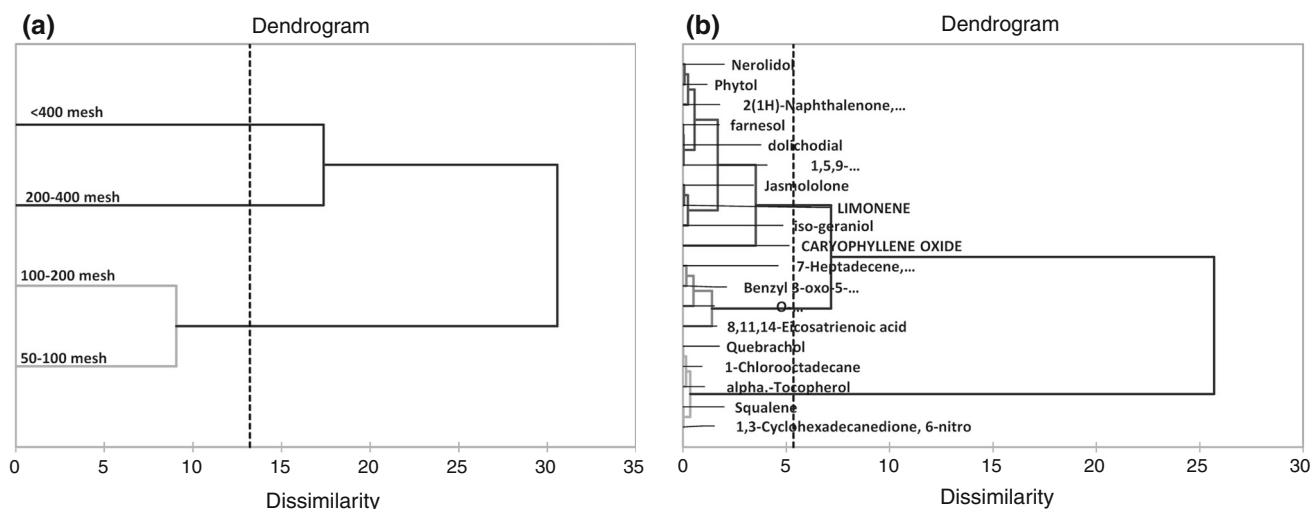


Fig. 10 Dendrograms obtained by HCA of pyrolysis data from the *P. pyramidalis* herbal drugs (a) and compounds (b) at 450 °C

compounds identified in the different herbal drugs and temperatures were studied through application of principal component analysis (PCA) and hierarchical cluster analysis (HCA). For all temperatures evaluated, the two first principal components (F1 and F2) were able to explain the variance between the herbal drugs, allowing to observe the special separation between them. The proximity between the compounds and the samples indicates that, for a given herbal drug, the closest substances were found in higher concentration, being the most representative of the respective samples. The HCA dendrograms allowed the observation of the samples clustering by their degree of similarity related to the concentration of the compounds, as well as the clustering of the compounds in each group according to their concentration.

Figure 5 shows the biplot of the samples and variables obtained from the PCA in 250 °C temperature. The two principal components analyzed (F1 and F2) accounted for 99.73% of the variance among the samples and were considered adequate to describe them. The samples 100–200 and 200–400 mesh were grouped together because of the similarity of their compounds concentration. The sample <400 mesh showed low representative of the peaks area at this temperature, but was shown to be close to the grouping previously mentioned. The herbal drugs and compounds were then grouped according to their similarity using the HCA, whose dendrograms are shown in Fig. 6. The sample 50–100 mesh proved to be the most different from all (Fig. 6a) because of poor similarity between their compounds and the others (Fig. 6b).

At the temperature of 350 °C (Fig. 7) were observed a greater amount of compounds directly related to the sample 50–100 mesh, making it few similar to the others (Fig. 8a). Despite having only two representative compounds in

common, samples 100–200 and 200–400 mesh were grouped together.

Figure 9 shows the biplot obtained by the PCA to the herbal drugs at the temperature of 450 °C. At this temperature, the two first principal orthogonal components explained slightly less correlation between data than at previous temperatures (87.91%). The samples 50–100 and 100–200 mesh presented many representative compounds in common, which probably allowed their grouping (Fig. 10a). The samples 200–400 and <400 mesh formed one second group, with low similarity to each other and even less about the other observed cluster. Compounds related to the sample <400 mesh were less similar to the other presented in the remaining herbal drugs (Fig. 10b).

Conclusions

The analytical methods used proved able to trace the characteristic profiles of herbal drugs from *P. pyramidalis*, highlighting differences related to the particle sizes of the same. Thermogravimetry pointed different mass losses in the thermal decomposition stages according to the atmosphere and the particle size. The kinetic of degradation presented different parameters values to each herbal drug, with energy activation and frequency factor decreasing in the smaller particle sizes. Differential thermal analysis showed distinct values of energy released at the thermal degradation processes of the different granulometric ranges. With the pyrolysis were evidenced some of the main compounds released during thermal degradation at different temperatures. The present study shows that the multivariate analysis PCA and HCA appears to be useful tools for the differentiation and classification of herbal drugs samples, even in different particle sizes, using the profile of

thermal degradation products obtained in the Pyr-GC/MS analysis. The physical and chemical characteristics allowed the distinction between different samples and providing parameters that can be used to prove the integrity and differentiation of each herbal drug.

References

1. Souza-Moreira TM, Salgado HRN, Pietro RCLR. O Brasil no contexto de controle de qualidade de plantas medicinais. *Rev Bras Farmacogn.* 2010;20:435–40.
2. Svetaz L, Zuljan F, Derita M, Petenatti E, Tamayo G, Cáceres A, et al. Value of the ethnomedical information for the discovery of plants with antifungal properties. A survey among seven Latin American countries. *J Ethnopharmacol.* 2010;127:137–58.
3. Oh SJ, Cho JH, Son CG. Systematic review of the incidence of herbal drug-induced liver injury in Korea. *J Ethnopharmacol.* 2015;159:253–6.
4. Santana DG, Santos CA, Santos ADC, Nogueira PCL, Thomazzi SM, Estevam CS, et al. Beneficial effects of the ethanol extract of *Caesalpinia pyramidalis* on the inflammatory response and abdominal hyperalgesia in rats with acute pancreatitis. *J Ethnopharmacol.* 2012;142:445–55.
5. Saraiva AM, Saraiva CL, Gonçalves AM, Soares RR, Mendes FO, Cordeiro RP, et al. Antimicrobial activity and bioautographic study of antistaphylococcal components from *Caesalpinia pyramidalis* Tull. *Braz J Pharm Sci.* 2012;48:147–54.
6. Ribeiro ARS, Diniz PBF, Estevam CS, Pinheiro MS, Albuquerque-Júnior RLC, Thomazzi SM. Gastroprotective activity of the ethanol extract from the inner bark of *Caesalpinia pyramidalis* in rats. *J Ethnopharmacol.* 2013;147:383–8.
7. Diniz PBF, Ribeiro ARS, Estevam CS, Bani CC, Thomazzi SM. Possible mechanisms of action of *Caesalpinia pyramidalis* against ethanol-induced gastric damage. *J Ethnopharmacol.* 2015;168:79–86.
8. Santos CA, Santos DS, Santana DG, Thomazzi SM. Evaluation of mechanisms involved in the antinociception of the ethanol extract from the inner bark of *Caesalpinia pyramidalis* in mice. *J Ethnopharmacol.* 2013;148:205–9.
9. Silva CHTP, Peixoto Sobrinho TJS, Saraiva AM, Pisciotano MNC, Amorim ELC. Phytochemical profile and antibacterial activity of bark and leaves of *Caesalpinia pyramidalis* Tul. and *Sapium glandulosum* (L.) Morong. *J Med Plants Res.* 2012;6:4766–71.
10. Kroes BH. The legal framework governing the quality of (traditional) herbal medicinal products in the European Union. *J Ethnopharmacol.* 2014;158:449–53.
11. Correia LP, Procópio JVV, Santana CP, Pinto MF, Moura EA, Santos AFO, et al. Herbal medicine physical quality evaluation by thermal analysis using adapted Ozawa method. *J Therm Anal Calorim.* 2015;122:207–14.
12. Correia PRM, Ferreira MMC. Reconhecimento de padrões por métodos não supervisionados: explorando procedimentos quimiométricos para tratamento de dados analíticos. *Quim Nova.* 2007;30:481–7.
13. Pan L, Dai F, Li G, Liu S. A TGA/DTA-MS investigation to the influence of process conditions on the pyrolysis of Jimsar oil shale. *Energy.* 2015;86:749–57.
14. Oliveira EJ, Alvarez EDA, Lima NGPB, Macedo RO. Usefulness of pyrolysis coupled to gas chromatography/mass spectrometry for evaluating the reproducibility of commercial samples of *Cymbopogon citratus* Stapf., Poaceae. *Rev Bras Farmacogn.* 2010;20:93–9.
15. Prata VM, Emídio ES, Doreá HS. Aplicação de métodos quimiométricos na caracterização de charutos utilizando a extração por dispersão da matriz em fase sólida e análise por cromatografia gasosa acoplada à espectrometria de massas. *Quim Nova.* 2011;34:53–8.